Mechanics of Materials 58 (2013) 12–22

Contents lists available at SciVerse ScienceDirect

Mechanics of Materials

journal homepage: www.elsevier.com/locate/mechmat

Analytical solutions for bilayered spherical hydrogel subjected to constant dilatation

Dong Wang, M.S. Wu *

School of Mechanical and Aerospace Engineering, 50 Nanyang Avenue, Nanyang Technological University, Singapore 639798

ARTICLE INFO

Article history:
Received 11 November 2011
Received in revised form 27 September 2012
Available online 19 November 2012

Keywords:
Bilayered hydrogels
Second-order elasticity
Dilatation

ABSTRACT

The application of multilayered hydrogel capsules in biomedical engineering has stimulated much interest in the mechanics of soft matter. Based on second-order elasticity theory, this paper presents analytical solutions for a spherically symmetric bilayered hydrogel subjected to a constant dilatation. The results show that: (1) elastic nonlinearity and inhomogeneity play a crucial role in the mechanical state, (2) a wide range of mechanical states can be designed for specific applications by manipulating the layer elasticity and interface position, and (3) the displacement and stresses can be characterized by a reduced set of eight geometric–elastic constants.

1. Introduction

There has been much interest in the development of hydrogels for applications in tissue engineering, stem cell technology and drug delivery. A consensus is emerging that the mechanical properties of hydrogels play a key role in such applications. For instance, polyacrylamide gel substrates with variable elastic moduli were used to culture human mesenchymal stem cells (hMSCs), and it was found that they differentiated predominantly into neurogenic, myogenic and osteogenic cells when cultured on substrates with elastic moduli in the range of 0.1–1 kPa, 8–17 kPa and 25–40 kPa, respectively (Engler et al., 2006). The increasingly large substrate moduli mimic those of the brain, muscle and bone, respectively. Similarly, studies of hMSCs on methacrylated hyaluronic acid hydrogels with moduli in the range of 3–100 kPa show that hMSCs exhibited enhanced proliferation on the stiffer gels and their behavior depended critically on the local elasticity (Marklein and Burdick, 2010).

Multilayered hydrogels are increasingly being explored for their great range of properties and increased functionalities, e.g., cultures of different cells can be carried out in the different layers of the gels. The layer-by-layer (LbL) technique for engineering planar and spherical hydrogels has been reviewed in recent works (Johnston et al., 2006; Detzel et al., 2011). In this technique, multilayered capsules are assembled by the alternate deposition of positively and negatively charged polyelectrolyte polymers. Facca et al. (2010) successfully employed polyelectrolyte multilayered capsules, composed of poly-L-glutamic acid and poly-L-lysine layers and embedded with active growth factors, for *in vivo* bone formation. Indeed, antibodies, drugs and nucleic acid can be encapsulated within or sandwiched between the layers. Furthermore, hydrogels respond to many stimuli such as pH, moisture and ionic strength and have found applications in diverse areas, e.g., actuators/sensors, bioseparations, food science and green technologies (Ehrick et al., 2005). A multilayered composition in such applications is highly beneficial as it enables the design of a tunable, multifunctional profile, e.g., mechanical strength, hydrophilicity and size exclusion (Johnson et al., 2010).

The investigation of the mechanical properties of hydrogels by the bioengineering and polymer chemistry communities has largely been restricted to the elastic modulus, e.g., Engler et al. (2006) and Marklein and Burdick (2010). This parameter, however, cannot capture the

* Corresponding author. Tel.: +65 6790 5545.
E-mail address: mmswu@ntu.edu.sg (M.S. Wu).

0167-6636/$ - see front matter © 2012 Elsevier Ltd. All rights reserved.
http://dx.doi.org/10.1016/j.mechmat.2012.11.001

nonlinear behavior of the soft material undergoing large deformation. Furthermore, biological processes may sense the substrate elasticity indirectly, through the stresses transferred to them. However, the nature, magnitude and distribution of the stresses in the hydrogel composites may not be easily computed. This motivates the present investigation of stresses in multilayered hydrogels.

For homogeneous soft materials, many types of constitutive models, e.g., molecular, microstructural and phenomenological, have been used to study the stress distributions, as reviewed by Wu (2011). Recently, a model for hydrogels, based on the free energies of polymer stretching and the mixing of water and polymer, was developed (Hong et al., 2008), and employed for solving a spherical gel problem (Zhao et al., 2008). Numerical treatment of the resulting differential equations was needed. Pursuing a different approach that emphasizes the material nonlinearity, Wu and Kirchner (2010) used the second-order elasticity theory of Murnaghan (1951) to study the mechanical response of biogels subjected to torsion, tension and shear. The model allows for the compressibility of the gels. They have also investigated the stresses in a single-layered spherical capsule subjected to a dilatation (Wu and Kirchner, 2011). The main advantages of the second-order elasticity approach are several. First, closed-form analytical solutions (although second-order) may be obtained, which in turn may reveal important physics missed by a complex model requiring numerical treatment, save computational time and avoid numerical convergence issues. Second, the acousto-elastic theory for measuring the elastic parameters in the second-order model is well-established and can be used to correlate with biological experimental data. Recently, Catheline et al. (2003) determined the second- and third-order elastic constants of a gelatin through measuring speed variations of shear waves as a function of applied stress. Moreover, the elastic constants can also be extracted by fitting the energy density in the Murnaghan theory to those in other theories, as demonstrated in Wu and Kirchner (2010). Third, the model, with a simple energy density function, can be incorporated in a large-scale numerical framework for handling irregular geometries and other complexities.

Higher order elasticity theories may also be used as constitutive models for biological soft tissues, including the effect of anisotropy, as investigated by Destrade et al. (2010). However, more elastic constants are needed in the higher order theories, although the assumption of incompressibility reduces the number of constants. For instance, third-order transversely isotropic compressible and incompressible theories require 29 and 13 elastic constants, respectively.

In this paper, we develop closed-form analytical solutions for the stresses and displacements in a bilayered spherical hydrogel subjected to a spherically symmetric dilatation. Emphasis is placed on investigating the influence of inhomogeneity arising from dissimilar layer elastic constants for achieving a wide spectrum of mechanical states. A dilatation may result from various fields such as temperature, concentration and pH. Kirchner (1974) studied the problem of precipitate coarsening in a linear elastic matrix, where the dilatation is a function of the precipitate concentration. As a first study, a constant dilatation is applied to the outer layer of the bilayered hydrogel. This may simulate the steady-state supply of nutrients to the outer layer only. Other spherically symmetric profiles can be chosen if needed.

The paper is organized in the following manner. In Section 2, the nonlinear elastic problem is defined and the solution approach is reviewed. In Section 3, the solutions are presented in detail. This is followed by numerical results in Section 4, a discussion in Section 5, and a set of conclusions in Section 6.

2. Nonlinear elastic model for dilatations

2.1. Definition of problem

Fig. 1 shows a spherical hydrogel consisting of an outer layer of inner and outer radii r_a and r_b, respectively, and an inner core of radius r_a. It is assumed that the outermost surface of the hydrogel is traction-free and the inner core-outer layer interface is perfectly bonded with no defects. The second-order elasticity theory of Murnaghan (1951) is used to model the elastic nonlinearity of the two layers. Two second-order elastic constants λ_i, μ_i and three third-order elastic constants l_i, m_i, n_i, where $i = 1, 2$ (denoting the inner core and outer layer respectively), are used in this theory. A dilatation of $\vartheta(r)$ is applied to the hydrogel, where r is the radial coordinate. In the current study, a constant dilatation of magnitude $\vartheta = \vartheta_0$ is applied to the outer layer only. The objective is to derive the displacement field and the stress field. To facilitate the derivations, the nonlinear elastic model of Murnaghan (1951) is briefly reviewed next.

2.2. Outline of nonlinear elastic model

The energy density W of Murnaghan (1951) is written as a function of the strain invariants J_1, J_2, J_3 of the Lagrangian strain $\mathbf{E}$:

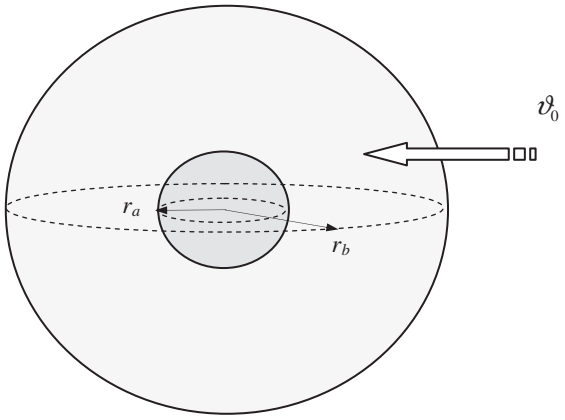

Fig. 1. A spherical hydrogel composite consisting of a core of radius r_a and an outer layer of outer radius r_b. A constant dilatation ϑ_0 is applied to the outer layer.

$$W=\frac{\lambda+2\mu}{2}J_1^2-2\mu J_2+\frac{l+2m}{3}J_1^3-2mJ_1J_2+nJ_3, \tag{2.1}$$

where λ, μ are the second-order and l, m, n the third-order elastic constants, respectively. In terms of the principal strains E_1, E_2 and E_3 of **E**, the three strain invariants take the following form:

$$J_1=E_1+E_2+E_3,\quad J_2=E_1E_2+E_2E_3+E_3E_1,\quad J_3=E_1E_2E_3. \tag{2.2}$$

The governing equation (the equilibrium equation in the radial direction) and the boundary condition on the outermost surface can be shown to be (Wu and Kirchner, 2011):

$$T_r'+\frac{2}{r}T_r-\frac{2}{r}T_\theta=-\rho F_r,\quad T_r(r=r_b)=0, \tag{2.3}$$

where T_r and T_θ are the radial and meridional (or azimuthal) components of the stress in the undeformed coordinate system, ρ is the mass density, and the force per unit volume ρF_r is a function of the dilatation:

$$\rho F_r=-k\left(\lambda+\frac{2}{3}\mu\right)\frac{d(3\vartheta)}{dr}+k^2\left(\lambda+\frac{2}{3}\mu-2l-\frac{2n}{9}\right)(3\vartheta)\frac{d(3\vartheta)}{dr}. \tag{2.4}$$

The symbols k and k^2 denote the first- and second-order terms, respectively. The derivation of the solutions to this equation is shown in Section 3.

3. Solutions

The first step is to rewrite the equilibrium equation, Eq. (2.3), in terms of the radial displacement u_r and its derivative u_r' with respect to r. This is a spherically symmetric problem and other displacement components are zero. According to the perturbation procedure of Murnaghan (1951), u_r is written as the sum of the first- and second- order parts u and w:

$$u_r=u+kw, \tag{3.1}$$

where k keeps track of the approximation order. The total radial displacement is the direct sum of the first- and second-order displacements; k being merely a marker. The replacement of u_r by $u + kw$ is to be made in all expressions for the purpose of derivation. Omitting the details, the stresses T_r and T_θ obtained through the differentiation of W with respect to **E**, take the following form:

$$T_r=kT_r^L+k^2T_r^{NL}, \tag{3.2}$$

where $T_r^L and T_r^{NL}$ are the linear and nonlinear radial stresses, respectively:

$$T_r^L=\lambda\left(u'+2\frac{u}{r}\right)+2\mu u',$$
$$T_r^{NL}=\begin{bmatrix}\lambda\left(\frac{3}{2}u'^2+2\frac{uu'}{r}+\frac{u^2}{r^2}\right)\\ +3\mu u'^2+l\left(u'+2\frac{u}{r}\right)^2+2m\left(u'^2-\frac{u^2}{r^2}\right)+n\frac{u^2}{r^2}\\ +\lambda\left(w'+2\frac{w}{r}\right)+2\mu w'\end{bmatrix}, \tag{3.3}$$

and

$$T_\theta=kT_\theta^L+k^2T_\theta^{NL}, \tag{3.4}$$

where T_θ^L and T_θ^{NL} are the linear and nonlinear meridional stresses, respectively:

$$T_\theta^L=\lambda\left(u'+2\frac{u}{r}\right)+2\mu\frac{u}{r},$$
$$T_\theta^{NL}=\begin{bmatrix}\lambda\left(\frac{1}{2}u'^2+\frac{uu'}{r}+3\frac{u^2}{r^2}\right)\\ +3\mu\frac{u^2}{r^2}+l\left(u'+2\frac{u}{r}\right)^2+2m\left(\frac{u^2}{r^2}-\frac{uu'}{r}\right)+n\frac{uu'}{r}\\ +\lambda\left(w'+2\frac{w}{r}\right)+2\mu\frac{w}{r}\end{bmatrix}. \tag{3.5}$$

The total stresses are again the direct sum of their linear and nonlinear components. The nonlinear stresses contain both u and w and their first-order derivatives. These stress expressions and the body force expression of Eq. (2.4) are substituted into Eq. (2.3).

Upon extracting the k term of Eq. (2.3), the first-order part can be written as:

$$(\lambda+2\mu)\left(u''+2\frac{u'}{r}-2\frac{u}{r^2}\right)=(3\lambda+2\mu)\frac{d\vartheta}{dr}, \tag{3.6}$$

which can be rewritten as:

$$\frac{d}{dr}\left[\frac{1}{r^2}\frac{d(r^2u)}{dr}\right]=L\frac{d\vartheta}{dr}, \tag{3.7}$$

where the dimensionless parameter L is given by:

$$L=\frac{3\lambda+2\mu}{\lambda+2\mu}=\frac{1+\nu}{1-\nu}, \tag{3.8}$$

with ν being the Poisson's ratio. The second-order equilibrium equation is associated with the k^2 term and can be written as:

$$\begin{aligned}&(\lambda+2\mu)\left(w''+2\frac{w'}{r}-2\frac{w}{r^2}\right)\\ &=-2(\lambda+3\mu+2m)\left[\left(u''+2\frac{u'}{r}-2\frac{u}{r^2}\right)u'-\frac{1}{r}\left(u'-\frac{u}{r}\right)^2\right]\\ &-(\lambda+2l)\left(u''+2\frac{u'}{r}-2\frac{u}{r^2}\right)\left(u'+2\frac{u}{r}\right)-\left(\lambda+\frac{2}{3}\mu-2l-\frac{2n}{9}\right)9\vartheta\frac{d\vartheta}{dr}.\end{aligned} \tag{3.9}$$

For a bilayered hydrogel, certain interface continuity conditions must be satisfied. In the following subsections, the solutions for the stresses and radial displacement are derived for the core (Material 1) and the outer layer (Material 2). For convenience, subscripts 1 and 2 are attached to the symbols for the stresses and displacements in these two materials, e.g., T_{1r}^L, T_{2r}^L, u_1, u_2, etc. Note also that the stresses in Eqs. (3.3) and (3.5) should be computed from $u_r/r-\vartheta$ and $u_r'-\vartheta$ (rather than u_r/r and u_r') as it is the difference between the fields that preserves the continuity of the body.

3.1. Solutions for Material 1

As stated previously, the core has the radius r_a and no dilatation is applied to it. To satisfy the interface boundary conditions, both the radial displacement and radial stress must be continuous across the interface at $r = r_a$. The linear and nonlinear parts of the solutions are derived below.

3.1.1. Linear part

Substitute $\vartheta = 0$ into Eq. (3.6). The solution to this first-order equation which fulfils a nonsingular u_1 at $r = 0$ is:

$$u_1 = A_1 r, \tag{3.10}$$

where A_1 is a dimensionless constant to be determined. Substituting u_1 into the linear stress expressions of Eqs. (3.3) and (3.5), the following explicit form for the stresses is obtained:

$$T^L_{1r} = T^L_{1\theta} = (3\lambda_1 + 2\mu_1)A_1. \tag{3.11}$$

3.1.2. Nonlinear part

Substitute $\vartheta = 0$ into Eq. (3.9) and the solution to the second-order equation which fulfils a nonsingular w_1 at $r = 0$ is:

$$w_1 = C_1 r, \tag{3.12}$$

where C_1 is a dimensionless constant to be determined. Substituting w_1 into the nonlinear stress expressions of Eqs. (3.3) and (3.5), the following explicit form is obtained:

$$T^{NL}_{1r} = T^{NL}_{1\theta} = \left(\frac{9}{2}\lambda_1 + 3\mu_1 + 9l_1 + n_1\right)A_1^2 + (3\lambda_1 + 2\mu_1)C_1. \tag{3.13}$$

From Eqs. (3.10) and (3.12), it can be observed that both the linear and nonlinear displacements of the core vary linearly with r. On the other hand, the core is subjected to a constant hydrostatic stress according to Eqs. (3.11) and (3.13).

3.2. Solutions for Material 2

The outer layer has the inner radius r_a and the outer radius r_b. A constant dilatation $\vartheta = \vartheta_0$ is applied to this layer. The following boundary conditions are enforced: the outermost surface $r = r_b$ is traction-free and the radial displacement and radial stress are continuous across the interface at $r = r_a$.

3.2.1. Linear part

Substituting $\vartheta = \vartheta_0$ into Eq. (3.6), the linear parts of the solutions for the radial displacement and the radial and meridional stresses in Material 2 can be obtained as:

$$u_2 = A_2 r + \frac{r_a^3}{r^2}B_2, \tag{3.14}$$

$$T^L_{2r} = (3\lambda_2 + 2\mu_2)\left(A_2 - \frac{L_2\vartheta_0}{3}\right) - \frac{4\mu_2 L_2\vartheta_0}{3} - \frac{4\mu_2 r_a^3}{r^3}B_2, \tag{3.15}$$

$$T^L_{2\theta} = (3\lambda_2 + 2\mu_2)\left(A_2 - \frac{L_2\vartheta_0}{3}\right) - \frac{4\mu_2 L_2\vartheta_0}{3} + \frac{2\mu_2 r_a^3}{r^3}B_2, \tag{3.16}$$

where A_2 and B_2 are dimensionless constants and $L_2 = (3\lambda_2 + 2\mu_2)/(\lambda_2 + 2\mu_2) = (1 + \nu_2)/(1 - \nu_2)$.

At this point, a total of four constants A_1, C_1, A_2, B_2 have appeared in the solutions. Application of the following boundary conditions

$$u_2(r_a) = u_1(r_a), \quad T^L_{2r}(r_a) = T^L_{1r}(r_a), \quad T^L_{2r}(r_b) = 0, \tag{3.17}$$

which respectively refer to the continuity of radial displacement and radial stress, and vanishing traction on the outermost surface, three of the constants A_1, A_2, B_2 can be determined:

$$A_1 = -\frac{4(r_a^3 - r_b^3)\vartheta_0\mu_2(3\lambda_2 + 2\mu_2)}{M}, \tag{3.18}$$

$$A_2 = \frac{\vartheta_0(3\lambda_2 + 2\mu_2)(-4\mu_2 r_a^3 + (3\lambda_1 + 2\mu_1 + 4\mu_2)r_b^3)}{M}, \tag{3.19}$$

$$B_2 = -\frac{\vartheta_0(3\lambda_1 + 2\mu_1)(3\lambda_2 + 2\mu_2)r_b^3}{M}, \tag{3.20}$$

where

$$M = 4\mu_2(3\lambda_1 - 3\lambda_2 + 2\mu_1 - 2\mu_2)r_a^3 + (3\lambda_2 + 2\mu_2) \times (3\lambda_1 + 2\mu_1 + 4\mu_2)r_b^3. \tag{3.21}$$

3.2.2. Nonlinear part

Substituting u_2 from Eq. (3.14) into Eq. (3.9), i.e., the second-order radial equilibrium equation, yields a differential equation in the variable w_2:

$$(\lambda_2 + 2\mu_2)\left(w_2'' + 2\frac{w_2'}{r} - 2\frac{w_2}{r^2}\right) = 18(\lambda_2 + 3\mu_2 + 2m_2)B_2^2\frac{r_a^6}{r^7}, \tag{3.22}$$

where a constant dilatation $\vartheta = \vartheta_0$ has been assumed. Eq. (3.22) has the solution:

$$w_2 = C_2 r + \frac{D_2 r_a^3}{r^2} + \frac{H_2 r_a^6}{r^5}, \tag{3.23}$$

where C_2, D_2, H_2 are all dimensionless constants. The last constant takes the form

$$H_2 = \frac{\lambda_2 + 3\mu_2 + 2m_2}{\lambda_2 + 2\mu_2}B_2^2, \tag{3.24}$$

and C_1 (which appears in Eq. (3.12)), C_2 and D_2 can be determined from the boundary conditions, which are the nonlinear counterparts to Eq. (3.17):

$$w_2(r_a) = w_1(r_a), \quad T^{NL}_{2r}(r_a) = T^{NL}_{1r}(r_a), \quad T^{NL}_{2r}(r_b) = 0. \tag{3.25}$$

Using Eq. (3.23) for w_2 and the nonlinear part of Eq. (3.3) for T^{NL}_{2r}, the constants C_1, C_2 and D_2 are determined to be:

$$C_1 = \frac{1}{2r_b^3 M}(\xi_1 r_a^6 + \xi_2 r_a^3 r_b^3 + \xi_3 r_b^6), \tag{3.26}$$

$$C_2 = -\frac{1}{2(\lambda_2 + 2\mu_2)r_b^3 M}(\xi_4 r_a^6 + \xi_5 r_a^3 r_b^3 + \xi_6 r_b^6), \tag{3.27}$$

$$D_2 = \frac{1}{M r_b^3}(\xi_7 r_a^6 + \xi_8 r_a^3 r_b^3 + \xi_9 r_b^6), \tag{3.28}$$

and ξ_i, $i = 1,2,\ldots,9$ are functions of the two sets of elastic constants given in Appendix A.

The second-order radial and meriodional stresses can be written out explicitly with the aid of the second parts of Eqs. (3.3) and (3.5):

$$T_{2r}^{NL} = \frac{1}{2(\lambda_2 + 2\mu_2)}\left(\zeta_1 + \frac{\zeta_2 r_a^3}{r^3} + \frac{\zeta_3 r_a^6}{r^6}\right), \tag{3.29}$$

$$T_{2\theta}^{NL} = \frac{1}{2(\lambda_2 + 2\mu_2)}\left(\zeta_1 - \frac{\zeta_2 r_a^3}{2r^3} - \frac{2\zeta_3 r_a^6}{r^6}\right), \tag{3.30}$$

where ζ_1, ζ_2, ζ_3 are also functions of the elastic constants and given in Appendix A.

From these results for Material 2, it can be seen that the displacement and stresses assume the form of a power-law. Specifically, the linear part of the displacement is dependent on r and r^{-2}, while the nonlinear part is dependent on r, r^{-2} and r^{-5}. For the stresses, all the corresponding power law exponents are one degree lower. The higher negative exponents for the nonlinear displacement and stresses imply that nonlinearity gains more influence as r becomes smaller. Moreover, the displacement expressions given in Eqs. (3.10), (3.12), (3.14), and (3.23) reveal that a reduced set of four geometric–elastic constants can completely characterize the displacement field. Similarly, the stresses given in Eqs. (3.11), (3.13), (3.15), (3.16), (3.29), and (3.30) can be characterized by another reduced set of four constants. The original material and geometric parameters consist of ten elastic constants and the radii r_a, r_b.

4. Numerical results

In summary, the analytical solutions for the linear parts of the radial displacement and radial and meridional stresses in Material 1 are given by Eqs. (3.10) and (3.11), respectively. The corresponding nonlinear parts are given by Eqs. (3.12) and (3.13). For Material 2, the corresponding equations are Eqs. (3.14)–(3.16) for the linear part and Eqs. (3.23), (3.29), and (3.30) for the nonlinear part. All numerical results below are obtained using these equations.

The dilatation is chosen to be 0.35. The ratio of the radii is chosen to be $r_b/r_a = 2$ in all the figures, except Fig. 5. The elastic constants are expressed in the units of NkT, where N is the number of polymer chains per unit volume of dry polymer, k the Boltzmann constant and T the absolute temperature. Typical values for NkT lie in the range 10^{-5} to 10^{-2} GPa. For ease of reference, the elastic constants used in the figures are summarized in Table 1. The following values $\lambda = 3570NkT$, $\mu = 1030\ NkT$, $l = -3560\ NkT$, $m = -2420\ NkT$ and $n = -2350\ NkT$, taken from Wu and Kirchner (2010), are chosen as the reference from which the variations are investigated. However, not only can the elastic constants vary over a wide range, but they can also be

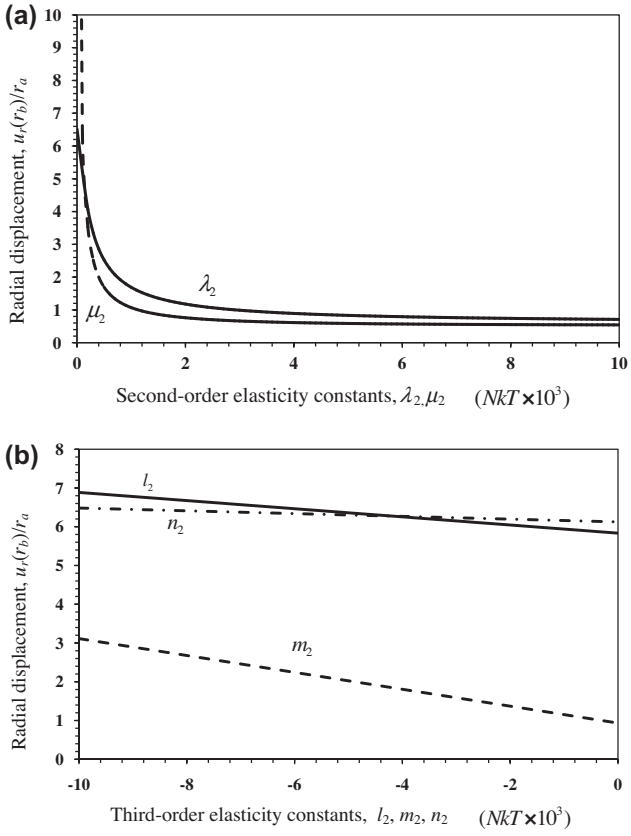

Fig. 2. Variation of the normalized radial displacement at the outer boundary with (a) second-order and (b) third-order elasticity parameters of Material 2 in a hydrogel composite.

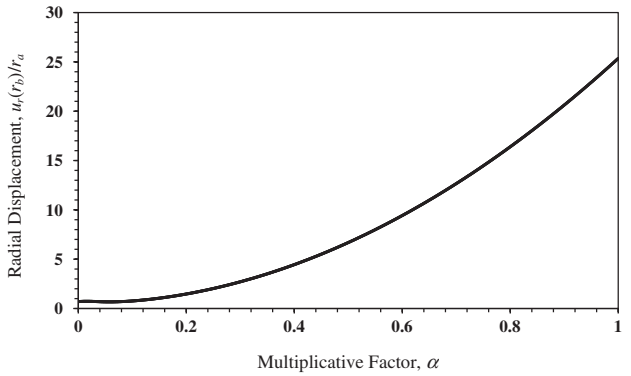

Fig. 3. Variation of the normalized radial displacement at the outer boundary with a multiplicative factor α.

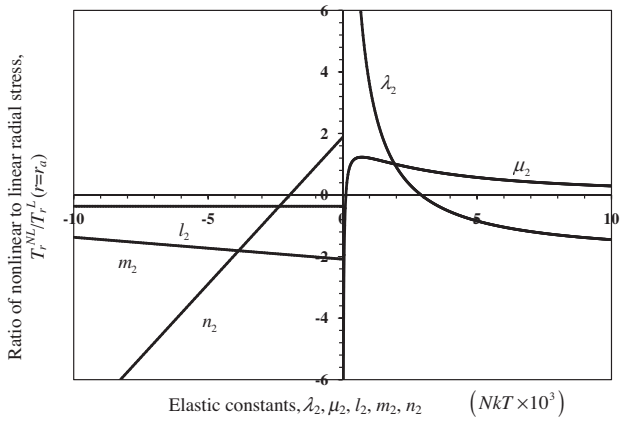

Fig. 4. Variation of the ratio of nonlinear to linear radial stress at the interface $r = r_a$ with λ_2, μ_2, l_2, m_2 and n_2 in a hydrogel composite.

orders of magnitude different from each other. For instance, the elastic modulus was varied over three orders of magnitude by manipulating the degree of polymer crosslinking (Engler et al., 2006; Marklein and Burdick, 2010). Also, Catheline et al. (2003) obtained the following values in kPa for agar–gelatin based phantoms via the method of transient elastography: λ (2.25×10^6), μ (6.35 to 9.67), l (-2×10^6 to 55×10^6), m (-26×10^6 to -12×10^6) and n (-101 to -64). The constant λ is five to six orders of magnitude larger than μ, while l and m are four to five orders of magnitude larger than n.

4.1. Influence of elastic constants on swelling behavior

Fig. 2(a) and (b) plot the dependence of $u_r(r = r_b)/r_a$ (the normalized radial displacement at the outer boundary) on the linear (λ_2, μ_2) and nonlinear (l_2, m_2, n_2) elastic constants, respectively. Table 1 shows the elastic constants selected for the simulations, where all elastic constants in Materials 1 take their reference values while those in Material 2 are fixed at the tabulated values except for the particular elastic constant that is being varied for each curve.

Several observations can be made. First, the radial displacement is nonlinearly dependent on the linear elastic constants, but linearly dependent on the nonlinear constants. This can be inferred from the relevant equations. It can also be observed from Fig. 2(a) that larger values of the second-order constants, i.e., λ_2 and μ_2, give rise to smaller swelling. In general, if a material has relatively large (small) values of the second-order constants, it is said to be "linearly hard (soft)". Furthermore, increasing the third-order elastic constant m_2 (negatively) increases substantially the swelling of the hydrogel composite, while varying l_2 and n_2 cause less change to the swelling, see Fig. 2(b). This shows that m_2 is the more dominating third-order parameter, which can be used to design the swelling characteristic of the composite. In general, if the magnitude of m for a material is large (small), it is said to be "nonlinearly soft (hard)".

Fig. 3 plots $u_r\,(r = r_b)/r_a$ against a multiplicative factor α, with $\lambda_1 = 35700\alpha$, $\mu_1 = 10300\alpha$, $l_1 = -3560$, $m_1 = -2420/\alpha$, $n_1 = -2350$; $\lambda_2 = 357/\alpha$, $\mu_2 = 103/\alpha$, $l_2 = -3560$, $m_2 = -242000\alpha$, $n_2 = -2350$. As α increases from 0 to 1, this implies that Material 1 becomes both linearly and nonlinearly hard, while Material 2 becomes both linearly and nonlinearly soft. For this range of variation, the ratio $u_r(r = r_b)/r_a$ increases 25-fold. Hence, it may be possible to control the swelling behavior to a large degree by properly designing the linear and nonlinear elasticity of the core and the outer layer.

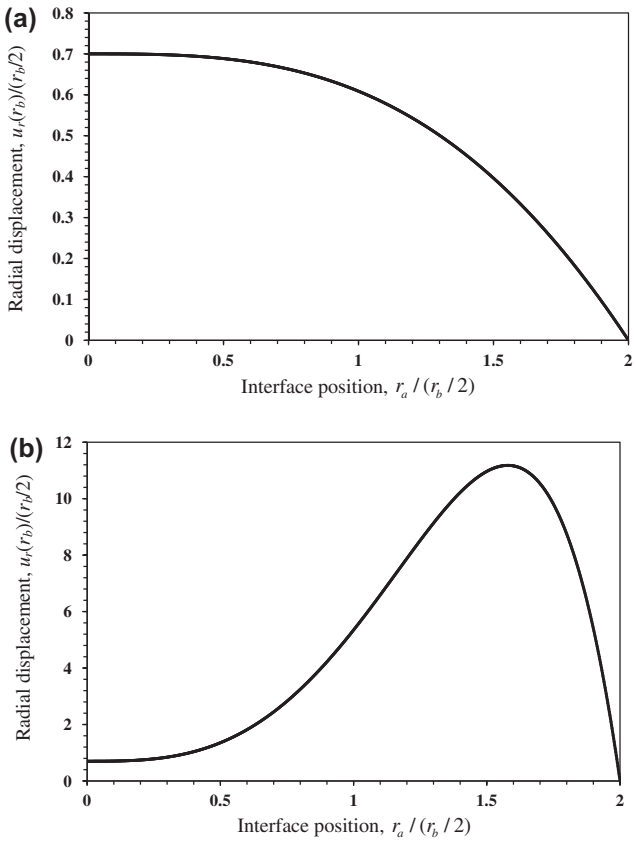

Fig. 5. Variation of the normalized surface radial displacement with interface position $r_a/(r_b/2)$ while keeping r_b fixed for different sets of elastic constants shown in Table 1: (a) Set 1, and (b) Set 2.

Table 1
Elastic constants for Figs. 2–7 (unit: *NkT*).

Figure	λ_1	μ_1	l_1	m_1	n_1	λ_2	μ_2	l_2	m_2	n_2
2a	3570	1030	−3560	−2420	−2350		103	−3560	−24200	−2350
	3570	1030	−3560	−2420	−2350	357		−3560	−24200	−2350
2b	3570	1030	−3560	−2420	−2350	357	103		−24200	−2350
	3570	1030	−3560	−2420	−2350	357	103	−3560		−2350
	3570	1030	−3560	−2420	−2350	357	103	−3560	−24200	
3	35700α	10300α	−3560	−2420/α	−2350	357/α	103/α	−3560	−242000α	−2350
4	35700	10300	−3560	−2420	−2350		103	−3560	−24200	−2350
	35700	10300	−3560	−2420	−2350	3570		−3560	−24200	−2350
	35700	10300	−3560	−2420	−2350	3570	103		−24200	−2350
	35700	10300	−3560	−2420	−2350	3570	103	−3560		−2350
	35700	10300	−3560	−2420	−2350	3570	103	−3560	−24200	
5a Set 1	3570	1030	−3560	−2420	−2350	3570	1030	−3560	−2420	−2350
5b Set 2	2.25×10^6	8	-2×10^6	-20×10^6	−100	2.25×10^5	8	-2×10^6	-20×10^6	−100
6a Set 1	0.00357	0.00103	−0.3560	−0.00242	−0.2350	3.5700	1.0300	−0.3560	−2.4200	−0.2350
6b Set 2	3.5700	1.0300	−0.3560	−2.4200	−0.2350	0.00357	0.00103	−0.3560	−0.00242	−0.2350
7	3.5700	1.0300	−0.3560	−0.00242	−0.2350	0.00357	0.00103	−0.3560	−2.4200	−0.2350

4.2. Ratio of nonlinear to linear radial stress

To explore the relative importance of nonlinear and linear effects, the ratio of nonlinear to linear radial stress at the interface $r = r_a$ is plotted against λ_2, μ_2, l_2, m_2 and n_2 in Fig. 4. The elastic constants in both the core and the shell are held fixed, except for the particular one being varied for each curve shown in the figure. Refer to Table 1 for the actual values.

The nonlinear part of the stress can be less than, comparable to, or larger than the linear part. For example, the ratio of the stresses exceeds 1 in the range $0 < \lambda_2 < 2000$ *NkT*. Also, the ratio can be negative, implying that the nonlinear and linear parts will add up to a smaller magnitude com-

pared to the larger magnitude of the two parts. Furthermore, the dependence of the ratio on the linear constants is non-monotonic, while its dependence on the nonlinear constants is linear. These results, however, are subject to the restriction of second-order theory. Overall, Fig. 4 suggests that the characterization of the mechanical property of a hydrogel by a single linear elastic constant in applications such as culturing stem cells on hydrogel substrates is unlikely to be accurate and may be misleading.

4.3. Influence of interface position

Fig. 5 plots $u_r(r = r_b)/(r_b/2)$ against $r_a/(r_b/2)$ with r_b fixed. Two cases are considered: homogeneous material in Fig. 5(a) and a composite in Fig. 5(b). As $r_a/(r_b/2)$ changes between 0 and 2, the interface changes its position from a location close to the spherical center to a location near to the outer surface. This means that when $r_a/(r_b/2)$ is close to zero, the composite is made up almost entirely of Material 2. The elastic constants chosen for the homogeneous hydrogel are their reference values, while those chosen for the composite are similar to those of Catheline et al. (2003). For the composite, the core is linearly hard while the shell is linearly soft ($\lambda_1/\lambda_2 = 10$, while all other corresponding constants assume the same values). It is also notable that the shear modulus $\mu_1 = \mu_2 = 8\ NkT$ is considerably smaller than all the other constants.

Fig. 5(a) shows that as the interface moves from the spherical center to the outer boundary, the swelling decreases monotonically. This is expected since the region in which the dilatation is applied, i.e., the outer layer, decreases in size. It can also be seen that the swelling is zero in the limit when the interface reaches the outer boundary. In contrast, Fig. 5(b) shows that the swelling first increases but subsequently decreases to zero with interface position, attaining a maximum value at $r_a/(r_b/2) \sim 1.6$. Also, the swelling in Fig. 5(b) is much more significant compared to that in Fig. 5(a) for $r_a/(r_b/2)$ between 0.5 and 1.8. The composite gel may thus offer a richer and more complex displacement profile that can be exploited for applications.

Further numerical simulations (omitted for brevity) reveal that that the stresses also vary significantly as the interface position changes. Hence, the swelling and internal stress characteristics of a hydrogel composite can be effectively controlled by varying the interface position, besides varying the elastic constants of the two layers.

4.4. Influence of elastic constants on stress state

In this section, smaller elastic constants of the order of 10^{-3} to 1 NkT are chosen for the hydrogel layers in order to mimic the elastic constants of cells or tissues. As stated in the Introduction, the mechanical properties of the sub-

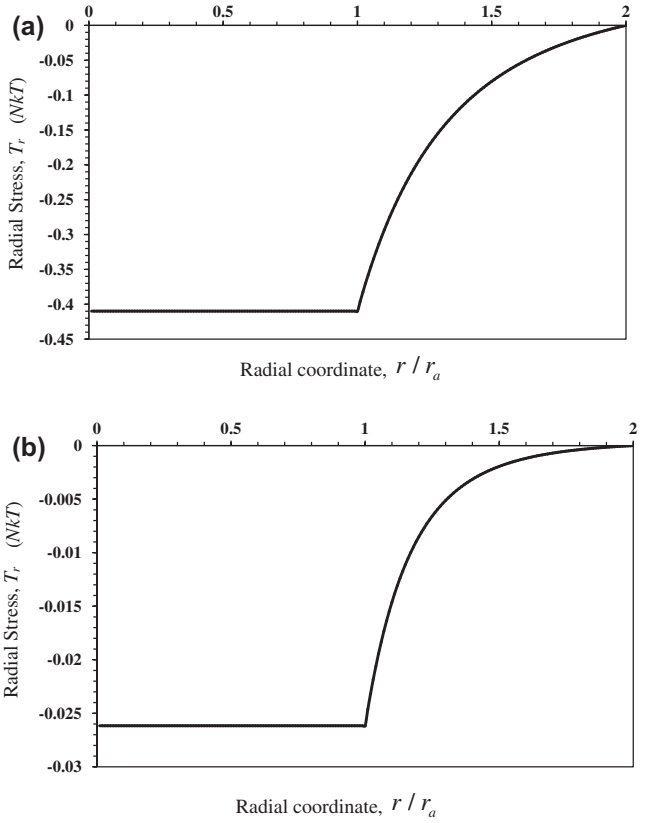

Fig. 6. Variation of the radial stress with the radial coordinate r/r_a for two different parameter sets: (a) large compressive radial stress (Set 1), and (b) smaller compressive radial stress (Set 2).

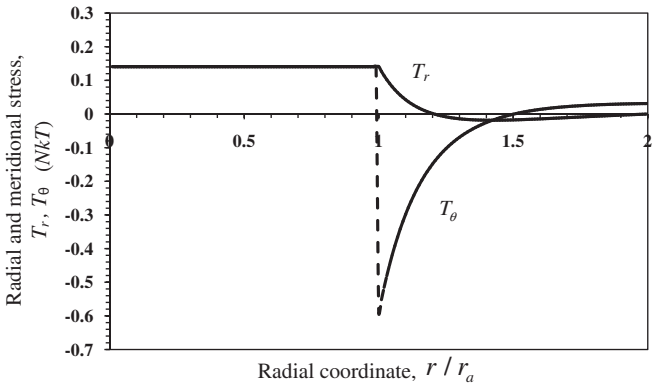

Fig. 7. Variation of the radial and meridional stresses with the radial coordinate r/r_a in a hydrogel composite.

strates for growing cells can control their growth characteristics.

Fig. 6 plots the radial stress T_r against the radial coordinate r/r_a for two different sets of elastic constants as indicated in Table 1. It can be seen that T_r is constant within the core as predicted by theory, is continuous across the interface as required by the continuity condition, and tends towards zero at the outer boundary, as required by the free-traction boundary condition. The compressive stress within the core reaches a value of ~ -0.41 NkT in Fig. 6(a), while it only reaches a value of ~ -0.026 NkT in Fig. 6(b). The value of -0.41 NkT is large compared to the order of the magnitude of the elastic constants. It may cause buckling instability of the hydrogel. Indeed, the buckling of a ring of tumor cells into various mode shapes has been investigated, e.g., Goriely and Ben Amar (2005).

Further numerical experiments confirm that the stresses inside the composite can also be tensile, depending on the elastic constants. The control of stress magnitude and sign is of significance in many applications; for example a large tensile stress may cause nucleation and extension of cracks in the material, or may influence the adherence and growth characteristics of tissues cultured on hydrogel substrates.

An important question remains as to the multiaxial stress state in the hydrogel that will have a direct bearing on biological processes. Fig. 7 plots the variation of T_r and T_θ with the normalized radial coordinate r/r_a. For this set of material parameters (see Table 1), the core experiences hydrostatic tension while the outer layer may experience triaxial tension–compression or triaxial compression. Hence, the use of a multilayered hydrogel allows much greater control of the stress state for applications in bioengineering.

5. Discussion

The work presented is based on second-order elasticity, characterized by five elastic constants. Analytical solutions for nonlinear composites are, generally speaking, not easily available, and hence the obtained power law expressions are a contribution that permits parametric studies and facilitates the observations of key physical trends. From the results in Section 4, we can make some assessments of the mechanical behavior of bilayered hydrogels as related to their elasticity, geometry and loading.

First, both the swelling and internal stresses can be manipulated via the judicious choice of the elasticity of the two layers. For instance, large swelling can be obtained by selecting a material characterized by a large negative value of the third-order constant m. It is also possible to make use of elastic inhomogeneity to elicit larger swelling compared to that obtainable with a homogeneous sphere of the same size.

Second, the material nonlinearity plays an essential role in the mechanical response. A very large range of values for the elastic constants can be exhibited by hydrogels of various types (e.g., pH, enzyme, electrical, temperature sensitive), dependent on factors such as chemical composition, methods of synthesis and cross-linking. Hence, the proper characterization of the three third-order constants in relation to mechanics-dependent biological processes is of great importance in designing bioenvironements.

Third, the mechanical behavior can also be effectively controlled via the selection of the relative thicknesses of the composite layers, i.e., the interface position. Various combinations of the interface position and the elastic parameters may be chosen to yield a composite with either large or negligible swelling, or one with the desired multiaxial stress state facilitating the intended functions.

Fourth, our theoretical results show that the mechanical behavior can be described by a total of only eight geometric–elastic constants, out of a total of 12 constants. This leads to greater flexibility in parameter selection, since the same mechanical state can be achieved by multiple parameter sets and the final choice can be made on the basis of other (non-mechanical) criteria.

Finally, it is emphasized that the loading on the composite sphere is caused by various concentrations, such as those due to drugs, proteins and growth factors, resulting in a dilatation field. The dilatation profile naturally plays a crucial role in the mechanical response. Hence, the design of the elasticity and layer thicknesses must also take into account the concentration profile within the composite.

Further possible issues and challenges are discussed in the following. An increasing number of theoretical and

experimental works on determining the nonlinear elastic constants of soft materials have been attempted, including those based on third-order elasticity (Gennisson et al., 2007; Rénier et al., 2008). This lays the foundation for solving multilayered soft materials using higher-order elasticity. However, the relationship between dilatation and the underlying physical phenomena (e.g., absorption of nutrients) should be explored. Kirchner (1974) considered various possible dilatation profiles in a linear elastic medium, but the relationship of these profiles to the contributing physical phenomena may be unclear.

The current work does not consider transient or time-dependent effects, which may be important for certain investigations such as cell proliferation on compliant substrates. Also, the existence of large compressive stresses in the hydrogel may induce buckling with potential adverse effects. Instability of nonlinear materials has been studied in a number of works (Sekimoto and Kawasaki, 1989; Haughton, 2004; Goriely and Ben Amar, 2005). Furthermore, only bilayered hydrogels are considered in this paper. Multilayered hydrogels have gained increasing importance, and generalization of the analytical solutions for a periodic multilayered hydrogel with alternate layers deserves future investigation.

The importance of interdisciplinary research should also be emphasized. While the bioengineers have characterized the mechanical property of the bioenvironment with a linear elastic modulus, much of the relationship between mechanical variables (such as stresses) and biological processes remains to be explored. For instance, it is not known how multiaxiality and sign of the stress state affect various biological processes. Some simulations have been attempted by the method of mechanics, e.g., the influence of cyclic substrate deformation on the growth orientation of endothelial cells (McGarry et al., 2005). Such computational studies were largely inspired by experimental investigations, e.g., Wang et al. (2001).

An interesting challenge is the computation of the isotropic effective moduli of a composite sphere. For a linear elastic medium containing a spherical inclusion, the effective bulk and shear moduli and their bounds have been studied previously, e.g., Hashin (1962) and Christensen and Lo (1979). In a later work, Herve and Zaoui (1993) derived the effective bulk and shear moduli of a linear elastic medium containing a multilayered spherical inclusion. An essential step in the derivation is the computation of the average strains and stresses in each phase based on the separation of hydrostatic and deviatoric components, and the use of a strain (or stress) condition which requires that the average strain (stress) in the n-layered sphere to be the same as the uniform macroscopic strain (stress) imposed at infinity. While a similar principle can be applied to nonlinear elastic spherical composites, additional works are anticipated. First, it is necessary to solve boundary value problems related to the imposition of hydrostatic pressure and simple shear; the shear problem is not solved in the current work. Second, determination of the effective third-order elastic constants would likely require the solution of additional boundary value problems, yet to be identified, since five effective parameters are to be determined. These problems will be addressed in the future.

In spite of the many outstanding issues, the current model represents a significant step towards the investigation of multilayered hydrogels. The obtained solutions have considered several essential elements: inhomogeneity arising from dissimilar layers, nonlinear elasticity and finite deformation. Incorporation of these elements has revealed the importance of nonlinearity in the elastic modeling of the hydrogel, the possible design of composite hydrogels based on dissimilar layer elasticity and the interface position, and the diverse range of hydrogel responses to even a simple dilatation.

6. Conclusions

Based on a second-order elasticity model, power law solutions have been obtained for a spherical hydrogel composite subjected to a dilatation. Two second- and three third-order elastic constants are used in the model. The dilatation is assumed to be constant and applied to the outer layer only.

The results show that nonlinearity is a significant part of the displacement and stresses, which can be completely characterized by a reduced set of eight geometric–elastic constants. Among the three nonlinear elastic parameters, m has a more dominant influence on the stresses and displacement compared to l and n. Studies are underway to investigate the relative importance of these parameters. Furthermore, a very wide range of swelling and multiaxial stress states are realizable by manipulating the layer elasticity and the layer thicknesses. Such results, in conjunction with experimental data, will help to elucidate the influence of microenvironment mechanical property on biological processes such as cell adhesion, proliferation and apoptosis.

Appendix A

The parameters appearing in Eqs. (3.26)–(3.28) are given explicitly as follows:

$$\xi_1 = 48B_2^2 m_2\mu_2 - 6B_2^2 n_2(\lambda_2+2\mu_2) + 6B_2^2\mu_2(\lambda_2+6\mu_2), \tag{A.1}$$

$$\begin{aligned}\xi_2 = {} & -48B_2^2 m_2\mu_2 - 4A_1^3(18l_1+2n_1+9\lambda_1+6\mu_1)\mu_2 \\ & + 6B_2^2 n_2(\lambda_2+2\mu_2) - 2B_2^2 n_2(3\lambda_2+2\mu_2) \\ & - 6B_2^2\mu_2(3\lambda_2+2\mu_2) - 6B_2^2\mu_2(\lambda_2+6\mu_2) \\ & + 4B_2(A_2-\vartheta_0)(3\lambda_2+2\mu_2)(6m_2-n_2+3\lambda_2+6\mu_2) \\ & + 4(A_2-\vartheta_0)^2\mu_2(18l_2+2n_2+9\lambda_2+6\mu_2),\end{aligned} \tag{A.2}$$

$$\begin{aligned}\xi_3 = {} & 2B_2^2 n_2(3\lambda_2+2\mu_2) - A_1^2(18l_1+2n_1+9\lambda_1+6\mu_1) \\ & \times(3\lambda_2+2\mu_2) + 6B_2^2\mu_2(3\lambda_2+2\mu_2) - 4B_2(A_2-\vartheta_0) \\ & \times(3\lambda_2+2\mu_2)(6m_2-n_2+3\lambda_2+6\mu_2) \\ & - 4(A_2-\vartheta_0)^2\mu_2(18l_2+2n_2+9\lambda_2+6\mu_2),\end{aligned} \tag{A.3}$$

$$\begin{aligned}\xi_4 = {} & 2B_2^2(3\lambda_1+2\mu_1+4\mu_2)(n_2(\lambda_2+2\mu_2) \\ & - \mu_2(8m_2+\lambda_2+6\mu_2)),\end{aligned} \tag{A.4}$$

$$\begin{aligned}\xi_5 = {} & 4(B_2\vartheta_0(3\lambda_1+2\mu_1)(\lambda_2+2\mu_2)(6m_2-n_2+3\lambda_2+6\mu_2)\\ & -A_2^2(\lambda_2+2\mu_2)\mu_2(18l_2+2n_2+9\lambda_2+6\mu_2)\\ & +2B_2^2\mu_2(-n_2\lambda_2+(2m_2+\lambda_2)(3\lambda_1+2\mu_1)\\ & +(8m_2-2n_2+9\lambda_1+\lambda_2+6\mu_1)\mu_2+6\mu_2^2)\\ & +\mu_2(\lambda_2+2\mu_2)(A_1^2(18l_1+2n_1+9\lambda_1+6\mu_1)\\ & -\vartheta_0^2(18l_2+2n_2+9\lambda_2+6\mu_2))+A_2(\lambda_2+2\mu_2)\\ & \times(-B_2(3\lambda_1+2\mu_1)(6m_2-n_2+3\lambda_2+6\mu_2)\\ & +2\vartheta_0\mu_2(18l_2+2n_2+9\lambda_2+6\mu_2))),\end{aligned} \tag{A.5}$$

$$\begin{aligned}\xi_6 = {} & (A_2-\vartheta_0)^2(\lambda_2+2\mu_2)(3\lambda_1+2\mu_1+4\mu_2)(18l_2\\ & +2n_2+9\lambda_2+6\mu_2),\end{aligned} \tag{A.6}$$

$$\begin{aligned}\xi_7 = {} & -\frac{1}{(\lambda_2+2\mu_2)}\Big(B_2^2(-3\lambda_1+3\lambda_2-2\mu_1+2\mu_2)\\ & \times\big(n_2(\lambda_2+2\mu_2)-\mu_2(8m_2+\lambda_2+6\mu_2)\big)\Big),\end{aligned} \tag{A.7}$$

$$\begin{aligned}\xi_8 = {} & 2B_2(A_2-\vartheta_0)(-3\lambda_1+3\lambda_2-2\mu_1+2\mu_2)\\ & \times(6m_2-n_2+3\lambda_2+6\mu_2),\end{aligned} \tag{A.8}$$

$$\begin{aligned}\xi_9 = {} & \left(\frac{9}{2}\lambda_2+3\mu_2+9l_2+n_2\right)(A_2-\vartheta_0)^2\\ & \times(-3\lambda_1+3\lambda_2-2\mu_1+2\mu_2)+(3\lambda_2+2\mu_2)\\ & \times\left(A_1^2\left(\frac{9}{2}\lambda_1+3\mu_1+9l_1+n_1\right)+\frac{1}{2(\lambda_2+2\mu_2)}\right.\\ & \times(4B_2(A_2-\vartheta_0)(\lambda_2+2\mu_2)(6m_2-n_2+3\lambda_2+6\mu_2)\\ & -(A_2-\vartheta_0)^2(\lambda_2+2\mu_2)(18l_2+2n_2+9\lambda_2+6\mu_2)\\ & +2B_2^2(-n_2\lambda_2+(2m_2+\lambda_2)(3\lambda_1+2\mu_1)\\ & \left.+(8m_2-2n_2+9\lambda_1+\lambda_2+6\mu_1)\mu_2+6\mu_2^2))\right).\end{aligned} \tag{A.9}$$

Finally, the parameters appearing in Eqs. (3.29) and (3.30) are given by:

$$\begin{aligned}\zeta_1 = {} & \big(6C_2\lambda_2+\vartheta_0^2(18l_2+2n_2+9\lambda_2)\big)(\lambda_2+2\mu_2)\\ & +2\big(2C_2+3\vartheta_0^2\big)\mu_2(\lambda_2+2\mu_2)+A_2^2(\lambda_2+2\mu_2)\\ & \times(18l_2+2n_2+9\lambda_2+6\mu_2)-2A_2\vartheta_0(\lambda_2\\ & +2\mu_2)(18l_2+2n_2+9\lambda_2+6\mu_2),\end{aligned} \tag{A.10}$$

$$\begin{aligned}\zeta_2 = {} & -8D_2\mu_2(\lambda_2+2\mu_2)-4A_2B_2(\lambda_2+2\mu_2)\\ & \times(6m_2-n_2+3\lambda_2+6\mu_2)+4B_2\vartheta_0(\lambda_2+2\mu_2)\\ & \times(6m_2-n_2+3\lambda_2+6\mu_2),\end{aligned} \tag{A.11}$$

$$\zeta_3 = 2B_2^2(n_2(\lambda_2+2\mu_2)-\mu_2(8m_2+\lambda_2+6\mu_2)). \tag{A.12}$$

References

Catheline, S., Gennisson, J.L., Fink, M., 2003. Measurement of elastic nonlinearity of soft solid with transient elastography. J. Acoust. Soc. Am. 114, 3087–3091.

Christensen, R.M., Lo, K.H., 1979. Solutions for effective shear properties in three phase sphere and cylinder models. J. Mech. Phys. Solids 27, 315–330.

Destrade, M., Gilchrist, M.D., Ogden, R.W., 2010. Third- and fourth-order elasticities of biological soft tissues. J. Acoust. Soc. Am. 127, 2103–2106.

Detzel, C.J., Larkin, A.L., Rajagopalan, P., 2011. Polyelectrolyte multilayers in tissue engineering. Tissue Eng. Part B 17, 101–113.

Ehrick, J.D., Deo, S.K., Browning, T.W., Bachas, L.G., Madou, M.J., Daunert, S., 2005. Genetically engineered protein in hydrogels tailors stimuli-responsive characteristics. Nature Mater. 4, 298–302.

Engler, A.J., Sen, S., Sweeney, H.L., Discher, D.E., 2006. Matrix elasticity directs stem cell lineage specification. Cell 126, 677–689.

Facca, S., Cortez, C., Mendoza-Palomares, C., Messadeq, N., Dierich, A., Johnston, A.P., et al., 2010. Active multilayered capsules for in vivo bone formation. Proc. Natl. Acad. Sci. USA 107, 3406–3411.

Gennisson, J.L., Renier, M., Catheline, S., Barriere, C., Bercoff, J., Tanter, M., et al., 2007. Acoustoelasticity in soft solids: assessment of the nonlinear shear modulus with the acoustic radiation force. J. Acoust. Soc. Am. 122, 3211–3219.

Goriely, A., Ben Amar, M., 2005. Differential growth and instability in elastic shells. Phys. Rev. Lett. 94, 198103.

Haughton, D.M., 2004. On non-linear stability in unconstrained non-linear elasticity. Int. J. Nonlinear Mech. 39, 1181–1192.

Hashin, Z., 1962. The elastic moduli of heterogeneous materials. J. Appl. Mech. 29, 143–150.

Herve, E., Zaoui, A., 1993. *N*-layered inclusion-based micromechanical modeling. Int. J. Eng. Sci. 31, 1–10.

Hong, W., Zhao, X.H., Zhou, J.X., Suo, Z.G., 2008. A theory of coupled diffusion and large deformation in polymeric gels. J. Mech. Phys. Solids 56, 1779–1793.

Johnson, L.M., Deforest, C.A., Pendurti, A., Anseth, K.S., Bowman, C.N., 2010. Formation of three-dimensional hydrogel multilayers using enzyme-mediated redox chain initiation. ACS Appl. Mater. Interface 2, 1963–1972.

Johnston, A.P.R., Cortez, C., Angelatos, A.S., Caruso, F., 2006. Layer-by-layer engineered capsules and their applications. Curr. Opin. Colloid Interface Sci. 11, 203–209.

Kirchner, H.O.K., 1974. Elastic behavior of a spherically symmetric concentration fluctuation in a finite body. Acta Metall. Mater. 22, 553–555.

Marklein, R.A., Burdick, J.A., 2010. Controlling stem cell fate with material design. Adv. Mater. 22, 175–189.

McGarry, J.P., Murphy, B.P., McHugh, P.E., 2005. Computational mechanics modelling of cell-substrate contact during cyclic substrate deformation. J. Mech. Phys. Solids 53, 2597–2637.

Murnaghan, F.D., 1951. Finite Deformation of an Elastic Solid. John Wiley, New York.

Rénier, M., Gennisson, J.L., Barriere, C., Royer, D., Fink, M., 2008. Fourth-order shear elastic constant assessment in quasi-incompressible soft solids. Appl. Phys. Lett. 93.

Sekimoto, K., Kawasaki, K., 1989. Elastic instabilities and phase coexistence of gels. Phys. A 154, 384–420.

Wang, J.H.-C., Goldschmidt-Clermont, P., Willie, J., Yin, F.C.-P., 2001. Specificity of endothelial cell reorientation in response to cyclic mechanical stretching. J. Biomech. 34, 1563–1572.

Wu, M.S., 2011. Strategies and challenges for the mechanical modeling of biological and bio-inspired materials. Mat. Sci. Eng. C 31, 1209–1220.

Wu, M.S., Kirchner, H.O.K., 2010. Nonlinear elasticity modeling of biogels. J. Mech. Phys. Solids 58, 300–310.

Wu, M.S., Kirchner, H.O.K., 2011. Second-order elastic solutions for spherical gels subjected to spherically symmetric dilatation. Mech. Mater. 43, 721–729.

Zhao, X.H., Hong, W., Suo, Z.G., 2008. Inhomogeneous and anisotropic equilibrium state of a swollen hydrogel containing a hard core. Appl. Phys. Lett. 92, 23.